

Significantly Reduced Thermal Conductivity in β -(Al_{0.1}Ga_{0.9})₂O₃/Ga₂O₃ Superlattices

Zhe Cheng,¹ Nicholas Tanen,² Celesta Chang,³ Jingjing Shi,¹ Jonathan McCandless,⁴ David Muller,^{5,6} Debdeep Jena,^{2,4,6} Huili Grace Xing,^{2,4,6} Samuel Graham,^{1,7, a)}

¹ George W. Woodruff School of Mechanical Engineering, Georgia Institute of Technology,
Atlanta, Georgia 30332, USA

² Department of Materials Science and Engineering, Cornell University, Ithaca, New York
14853, USA

³ Department of Physics, Cornell University, Ithaca, New York 14853, USA

⁴ School of Electrical and Computer Engineering, Cornell University, Ithaca, New York 14853,
USA

⁵ School of Applied and Engineering Physics, Cornell University, Ithaca, New York 14853, USA

⁶ Kavli Institute for Nanoscale Science, Cornell University, Ithaca, New York 14853, USA

⁷ School of Materials Science and Engineering, Georgia Institute of Technology, Atlanta,
Georgia 30332, USA

^{a)} Corresponding author: sgraham@gatech.edu

Abstract

β -Ga₂O₃ has emerged as a promising candidate for electronic device applications because of its ultra-wide bandgap, high breakdown electric field, and large-area affordable substrates grown from the melt. However, its thermal conductivity is at least one order of magnitude lower than that of other wide bandgap semiconductors such as SiC and GaN. Thermal dissipation in electronics made from β -Ga₂O₃ will be the bottleneck for real-world applications, especially for high power and high frequency devices. Similar to GaN/AlGaN interfaces, β -(Al_xGa_{1-x})₂O₃/Ga₂O₃ heterogeneous structures have been used to form a high mobility two-dimensional electron gas (2DEG) where joule heating is localized. The thermal properties of β -(Al_xGa_{1-x})₂O₃/Ga₂O₃ are the key for heat dissipation in these devices while they have not been studied before. This work reports the first measurement on thermal conductivity of β -(Al_{0.1}Ga_{0.9})₂O₃/Ga₂O₃ superlattices from 80 K to 480 K. Its thermal conductivity is significantly reduced (5.7 times reduction) at room temperature comparing with that of bulk Ga₂O₃. Additionally, the thermal conductivity of bulk Ga₂O₃ with (010) orientation is measured and found to be consistent with literature values regardless of Sn doping. We discuss the phonon scattering mechanism in these structures by calculating their inverse thermal diffusivity. By comparing the estimated thermal boundary conductance (TBC) of β -(Al_{0.1}Ga_{0.9})₂O₃/Ga₂O₃ interfaces and Ga₂O₃ maximum TBC, we reveal that some phonons in the superlattices transmit through several interfaces before scattering with other phonons or structural imperfections. This study is not only important for Ga₂O₃ electronics applications especially for high power and high frequency applications, but also for the fundamental thermal science of phonon transport across interfaces and in superlattices.

Introduction

As an emerging ultra-wide bandgap semiconductor material, β -Ga₂O₃ has shown promising properties for electronic device applications, such as an ultra-wide bandgap (4.8 eV) and high critical electric field (8 MV/cm), which predicts a Baliga figure of merit that is 3214 times that of Si.¹ However, the thermal conductivity of bulk β -Ga₂O₃ (10-30 W/m-K, depending on crystal orientation) is at least one order of magnitude lower than those of other wide bandgap semiconductors such as GaN (230 W/m-K), 4H-SiC (490 W/m-K), and diamond (>2000 W/m-K).^{2,3} Thermal dissipation will be the bottleneck for real-world applications, especially for high power and high frequency devices. Currently, compared to demonstrations of Ga₂O₃ devices, a disproportionately smaller number of thermal studies have been performed.⁴ Similar to GaN/AlGa_N interfaces, to demonstrate modulation-doped field effect transistors (MODFETs), β -(Al_xGa_{1-x})₂O₃/Ga₂O₃ heterogeneous structures have been used to form a high mobility two-dimensional electron gas (2DEG) where joule heating is localized.⁵⁻⁹ The thermal properties of the β -(Al_xGa_{1-x})₂O₃/Ga₂O₃ structure are the key for heat dissipation in these devices, however they have not been studied before.

In this work, we report the first measurement on temperature-dependent thermal conductivity of β -(Al_{0.1}Ga_{0.9})₂O₃/Ga₂O₃ superlattices epitaxial-grown on bulk (010) Ga₂O₃ substrates by molecular-beam epitaxy (MBE) from 80 K to 480 K. Multi-frequency time-domain thermoreflectance (TDTR) is used to measure the thermal properties of both the β -(Al_{0.1}Ga_{0.9})₂O₃/Ga₂O₃ superlattices and the bulk Ga₂O₃ substrates simultaneously. The phonon scattering mechanism in these structures is discussed in detail. Additionally, we estimate the

TBC of β -(Al_{0.1}Ga_{0.9})₂O₃/Ga₂O₃ interfaces and compare it with maximum Ga₂O₃ TBC. The mechanism of phonons transmission through interfaces is discussed.

Methods

The β -(Al_xGa_{1-x})₂O₃/Ga₂O₃ superlattice used in this study was homoepitaxy-grown on a Sn-doped (010) Ga₂O₃ substrate, with an n-type doping concentration of $4 \times 10^{18} \text{ cm}^{-3}$, using a Veeco Gen930 MBE system. The aluminum and gallium were provided by standard effusion cells. The oxygen plasma was produced using a Veeco RF plasma source. During the growth, the gallium and aluminum beam equivalent pressures (BEP) measured by an ion gauge were 1×10^{-8} Torr and 1×10^{-9} Torr, respectively. This led to an aluminum flux that is 9.1% of the total metal flux. The oxygen was flown into the chamber at 0.7 sccm and the RF plasma was struck using a load power of 289 W, which corresponded to a total chamber pressure of 2.18×10^{-5} Torr. The substrate temperature, measured by a thermocouple, was 500 °C for the entire growth. The substrate was mounted to a silicon carrier wafer using indium bonding. The substrate was grown by edge-defined film-fed growth (EFG) purchased from Novel Crystal Technology. The film has ten alternating periods of a Ga₂O₃ layer followed by a (Al_{0.1}Ga_{0.9})₂O₃ layer each grown for 30 minutes.

Cross-sectional TEM specimen was prepared using an FEI Strata 400 Focused Ion Beam (FIB) with a final milling step of 5keV to reduce surface damage. Atomic resolution high angle annular dark field (HAADF) images were acquired on an aberration corrected 300keV Themis Titan. The superlattice film thickness was determined by a scanning transmission electron microscopy (STEM) to be 114 nm, as shown in Figure 1. For each period, the Ga₂O₃ layer is about 6.5 nm thick while the (Al_{0.1}Ga_{0.9})₂O₃ layer is about 4.5 nm thick. The interfaces in the superlattice

structure are not very sharp. A layer of Al (~80 nm) was deposited on the surface as the TDTR transducer as demonstrated in several previous studies.¹⁰⁻¹⁴ A modulated pump beam heats the sample surface periodically while a delayed probe beam detects the surface temperature variation via thermoreflectance. The measured signal of temperature variation is fit with an analytical heat transfer solution to infer unknown parameters. Here, we measure one spot on the sample with two modulation frequencies, i.e., 3.6 MHz and 8.8 MHz, at room temperature. TDTR signal is sensitive to the thermal conductivity of the bulk Ga₂O₃ substrate with modulation frequency of 3.6 MHz while it is sensitive to the thermal conductivity of the superlattice with modulation frequency of 8.8 MHz. More details about multi-frequency TDTR measurements can be found in references.^{10,15-17} Additionally, we estimate the error bars here as $\pm 10\%$.

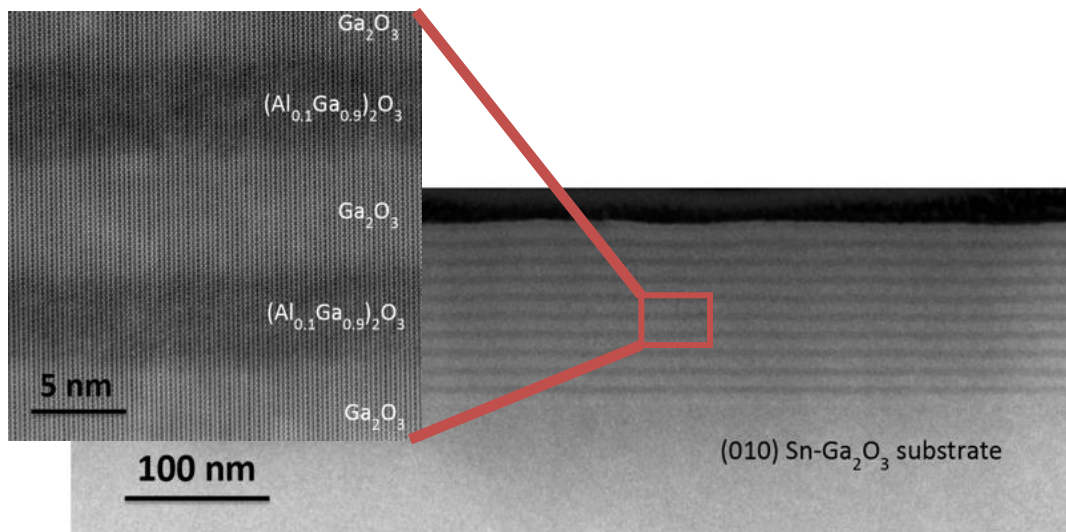


Figure 1. HAADF-STEM images of the β -(Al_{0.1}Ga_{0.9})₂O₃/Ga₂O₃ superlattice structure.

Results and Discussion

The temperature-dependent thermal conductivity of the bulk (010) Ga₂O₃ substrate and the β -(Al_{0.1}Ga_{0.9})₂O₃/Ga₂O₃ superlattice are shown in Figure 2 (a). At room temperature, the thermal

conductivity of the superlattice is 5.7 times smaller than that of the bulk (010) Ga₂O₃ substrate. This significantly reduced thermal conductivity further impedes thermal dissipation, potentially creating additional challenges for gallium oxide electronics devices. Aggressive thermal management techniques need to be applied for reliable device performance, such as integrating high thermal conductivity materials close to the regions where heat is being generated to aid in pulling out the heat. For the bulk (010) Ga₂O₃ substrate, its thermal conductivity decreases with increasing temperature from 80 K to 450 K because of increased phonon-phonon scattering. As temperature increases, the number of excited phonons increases, resulting in increasingly extensive phonon-phonon scatterings. For the superlattice, its thermal conductivity shows a peak at 380 K. Below 380 K, the thermal conductivity decreases with decreasing temperature while it decrease with increasing temperature above 380 K. For temperatures below 380 K, phonon-structural imperfection scattering, such as alloy and boundary, dominates in impeding thermal transport. For temperatures above 380 K, phonon-phonon scattering dominates. More about the scattering mechanisms will be discussed later.

The measured thermal conductivity of the bulk (010) Ga₂O₃ substrate is compared with literature values as shown in Figure 2 (b). Our measured values are consistent with most of other experimentally measured values and first-principle calculated values in the literature. This indicates that the Sn doping and unintentional doping do not affect the thermal conductivity significantly. The other samples measured in the literature have different levels of doping as well. It is still an open question as to how high doping concentrations would affect the thermal conductivity in β -Ga₂O₃.

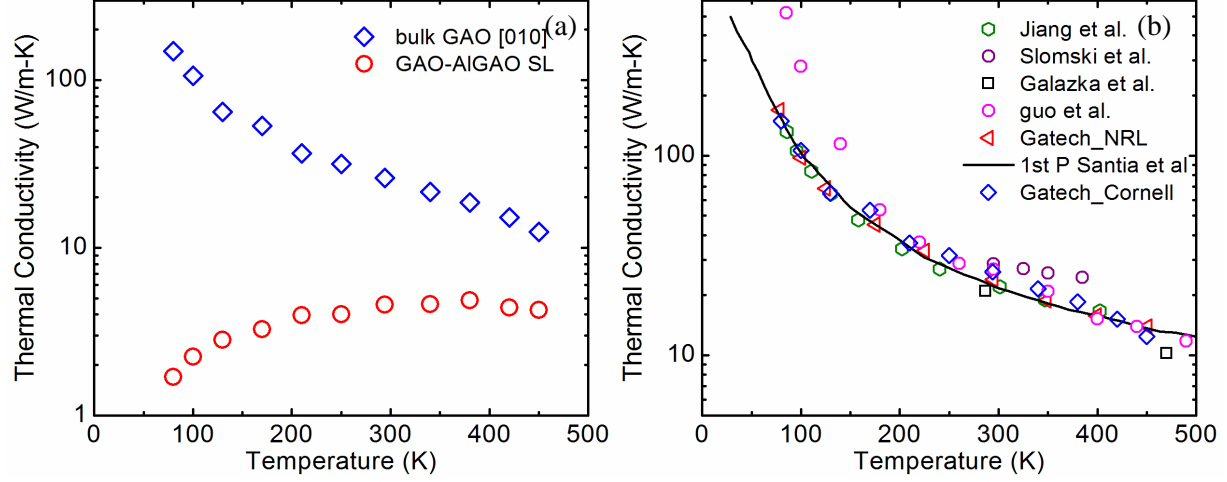


Figure 2. (a) Temperature-dependent thermal conductivity of the bulk Ga_2O_3 substrate and β - $(\text{Al}_{0.1}\text{Ga}_{0.9})_2\text{O}_3/\text{Ga}_2\text{O}_3$ superlattices. (b) Summary of temperature-dependent thermal conductivity of bulk (010) β - Ga_2O_3 in this work and literature.¹⁸⁻²⁰

To better understand the phonon scattering mechanism in the superlattice and bulk Ga_2O_3 , we calculate the inverse thermal diffusivity of both the superlattice and bulk Ga_2O_3 , as shown in Figure 3 (a). The formula of inverse thermal diffusivity is shown as below:

$$\frac{C_v}{k}(T) = \left\{ \sum_{n=1}^n \int_0^{\omega_D} g(\omega) k_B \left(\frac{\hbar\omega}{k_B T} \right)^2 e^{\frac{\hbar\omega}{k_B T}} / (e^{\frac{\hbar\omega}{k_B T}} - 1)^2 d\omega \right\} / \left\{ \sum_{n=1}^n \int_0^{\omega_D} g(\omega) k_B \left(\frac{\hbar\omega}{k_B T} \right)^2 e^{\frac{\hbar\omega}{k_B T}} / (e^{\frac{\hbar\omega}{k_B T}} - 1)^2 v_\omega^2 \left(\frac{1}{\tau_{ph}} + \frac{1}{\tau_{struc}} \right)^{-1} d\omega \right\}. \quad (1)$$

Here, C_v is the volumetric heat capacity, k is thermal conductivity, T is temperature, n is the number of phonon branches, ω_D is Debye frequency, $g(\omega)$ is phonon density of states, k_B is Boltzmann constant, \hbar is reduced Planck constant, ω is the phonon frequency, v_ω is the phonon group velocity, τ_{ph} is the relaxation time for phonon-phonon scattering, and τ_{struc} is the relaxation time for phonon-structural imperfection scattering. To the first-order approximation,

the inverse thermal diffusivity can be used to estimate the relative contribution of scattering sources.^{21,22} The temperature-dependent thermal conductivity of the superlattice and bulk Ga₂O₃ have different trends with temperature because of the strong temperature dependence of heat capacity. As a result, it is difficult to compare the contribution of phonon-phonon scattering and phonon-structural imperfection scattering according to the thermal conductivity data. After removing the effect of heat capacity, the inverse thermal diffusivity represents the relative contributions of phonon scattering sources qualitatively. As shown in Figure 3 (a), the inverse thermal diffusivity decreases with decreasing temperature because of reduced scattering intensity of phonon-phonon scattering. As temperature goes to zero, phonon-phonon scatterings diminish and only structural imperfection scatterings remain. Then Equation (1) can be simplified as:

$$\frac{c_v}{k}(T \rightarrow 0 \text{ K}) \approx \frac{3}{v_0^2 \tau_{struct}} = \frac{3}{v_0 l_0}. \quad (2)$$

Here, v_0 is the average phonon group velocity and l_0 is the scattering length arising from structural imperfections. For the bulk Ga₂O₃, the structural imperfection is negligible so nearly zero residual value is observed at low temperatures. However, a large residual value is observed at low temperatures for the superlattice, indicating strong structural imperfection scatterings, such as alloy scattering, boundary scattering, and point defect scattering. We estimate the average acoustic phonon group velocity as 2420 m/s.²⁰ Based on the residual inverse thermal diffusivity (40 s/cm²), the structural scattering length l_0 can be calculated as 3.1 nm, which is close to the layer thickness of the superlattice by considering additional alloy scatterings. The rough interfaces in the superlattice may reduce the effective thermal conductivity because the roughness at the interfaces may induce additional phonon scatterings.²³

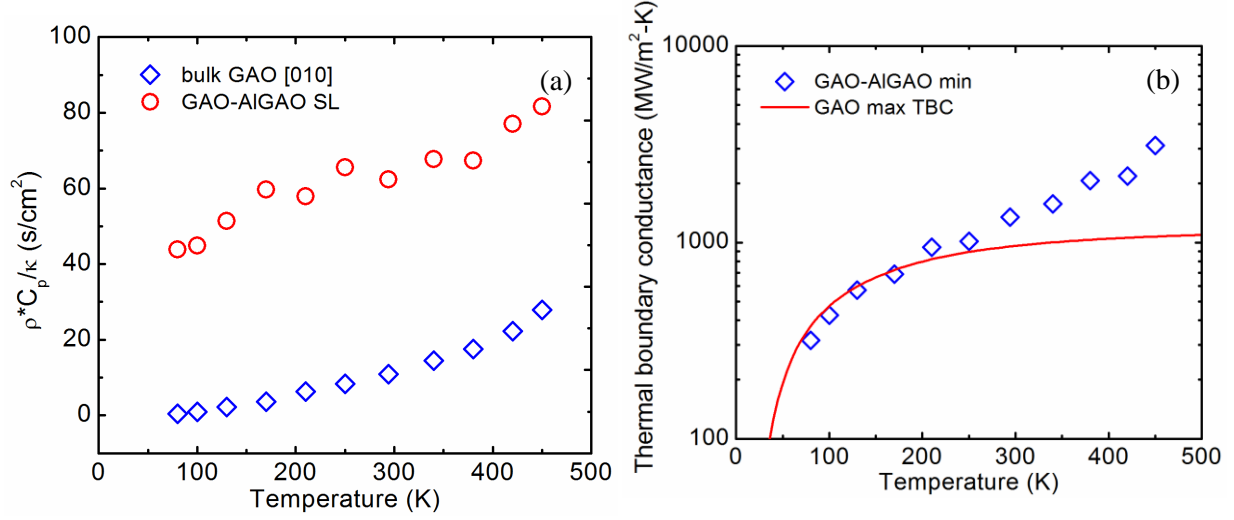


Figure 3. (a) Temperature-dependent inverse thermal diffusivity of bulk (010) Ga₂O₃ and β -(Al_{0.1}Ga_{0.9})₂O₃/Ga₂O₃ superlattices. (b) Temperature dependence of estimated minimum TBC (lower bound) of β -(Al_{0.1}Ga_{0.9})₂O₃ and Ga₂O₃ interfaces and maximum TBC of Ga₂O₃.

To understand the mechanism of phonons transmission through (Al_{0.1}Ga_{0.9})₂O₃/Ga₂O₃ interfaces, we estimate the TBC as below:

$$\frac{d_1}{k_{GAO}} + \frac{d_2}{k_{AIGAO}} + \frac{2}{TBC} = \frac{d_1 + d_2}{k_{measured}}. \quad (3)$$

Here, d_1 and d_2 are the thicknesses of the Ga₂O₃ layer and the (Al_{0.1}Ga_{0.9})₂O₃ layer in one period. k_{GAO} and k_{AIGAO} are the thermal conductivity of the Ga₂O₃ layer and the (Al_{0.1}Ga_{0.9})₂O₃ layer. TBC in this case refers to the TBC of the (Al_{0.1}Ga_{0.9})₂O₃/Ga₂O₃ interface. $k_{measured}$ is the measured effective thermal conductivity of the superlattice. k_{GAO} and k_{AIGAO} are supposed to be much lower than the bulk thermal conductivity because of boundary scattering and alloy scatterings. Here, we only consider the size effect resulting from total superlattice thickness (114 nm), the thermal conductivity reduces to 45% according to first-principle calculations.²⁰ As a result, the minimum TBC of the (Al_{0.1}Ga_{0.9})₂O₃/Ga₂O₃ interface could be estimated by assuming k_{GAO} and k_{AIGAO} as

bulk values only with size effect from the total thickness. To compare with this estimated TBC, we also calculate the max TBC of any heterogeneous interfaces which involving Ga_2O_3 . This max TBC is calculated by assuming the phonon transmission coefficient across the interface as unity (all phonons from Ga_2O_3 could transmit through the interface). As shown in Figure 3 (b), the estimated minimum TBC is larger than the max TBC of Ga_2O_3 interfaces, especially at high temperatures. At 450 K, the minimum TBC is almost three times larger than the max Ga_2O_3 TBC. This means that some phonons transmit through several interfaces before scattering with other phonons or structural imperfections. Here, the estimated TBC is the thermal energy transmitted across the interface for a certain temperature difference per unit area. Because the period of the superlattice is very small comparing with some long mean free path phonons, some phonons could transmit several interfaces without scattering with other phonons and structural imperfections. The energy of these phonons are accounted repeatedly for several times, resulting in a very large effective TBC, even larger than the max TBC Ga_2O_3 hetero-interfaces could achieve. This non-local and non-equilibrium phonon transport across interfaces is one of the challenges to define local temperature and understand thermal transport across interfaces. Similar phenomenon was observed in AlN-GaN superlattices before.²⁴ Our work is important since it may be necessary to design the superlattices not only for the creation of the channel 2DEG, but also for more efficient phonon dissipation through the structure. This electro-thermal co-design is truly an important feature for future wide bandgap devices which require enhancements in heat dissipation within the devices.

Conclusions

This work reports the first temperature-dependent measurement on thermal conductivity of β -(Al_{0.1}Ga_{0.9})₂O₃/Ga₂O₃ superlattices from 80 K to 480 K. We observed significantly reduced thermal conductivity (5.7 times reduction) at room temperature comparing with bulk Ga₂O₃. The thermal conductivity of bulk (010) Ga₂O₃ is measured and found to be consistent with literature values. By calculating the inverse thermal diffusivity of both the superlattice and bulk Ga₂O₃, we qualitatively identify the relative contribution of scattering intensity of phonon-phonon scattering and phonon-structural imperfection scattering. We estimated the scattering length as 3.1 nm, which is close to the layer thickness of the superlattice by considering additional alloy scatterings. The estimated minimum TBC of β -(Al_{0.1}Ga_{0.9})₂O₃/Ga₂O₃ interfaces is found to be larger than the Ga₂O₃ maximum TBC. This result shows that some phonons could transmit through several interfaces before scattering with other phonons or structural imperfections. This study is not only important for Ga₂O₃ electronics applications especially for high power and high frequency applications, but also for the fundamental thermal science of phonon transport across interfaces and in superlattices.

Acknowledgement

The authors would like to acknowledge the funding support from Air Force Office of Scientific Research under a MURI program (Grant No. FA9550-18-1-0479) and a Center of Excellence program (Grant No. FA9550-18-1-0529) and the Office of Naval Research under a MURI program (Grant No. N00014-18-1-2429).

References

- ¹ M. Higashiwaki and G. H. Jessen, (AIP Publishing, 2018).
- ² S. Pearton, J. Yang, P. H. Cary IV, F. Ren, J. Kim, M. J. Tadjer, and M. A. Mastro, *Applied Physics Reviews* **5**, 011301 (2018).
- ³ P. Jiang, X. Qian, X. Li, and R. Yang, arXiv preprint arXiv:1809.04762 (2018).
- ⁴ S. B. Reese, T. Remo, J. Green, and A. Zakutayev, *Joule* (2019).
- ⁵ S. Krishnamoorthy, Z. Xia, C. Joishi, Y. Zhang, J. McGlone, J. Johnson, M. Brenner, A. R. Arehart, J. Hwang, and S. Lodha, *Applied Physics Letters* **111**, 023502 (2017).
- ⁶ Y. Zhang, A. Neal, Z. Xia, C. Joishi, J. M. Johnson, Y. Zheng, S. Bajaj, M. Brenner, D. Dorsey, and K. Chabak, *Applied Physics Letters* **112**, 173502 (2018).
- ⁷ E. Ahmadi, O. S. Koksaldi, X. Zheng, T. Mates, Y. Oshima, U. K. Mishra, and J. S. Speck, *Applied Physics Express* **10**, 071101 (2017).
- ⁸ T. Oshima, Y. Kato, N. Kawano, A. Kuramata, S. Yamakoshi, S. Fujita, T. Oishi, and M. Kasu, *Applied Physics Express* **10**, 035701 (2017).
- ⁹ Y. Zhang, C. Joishi, Z. Xia, M. Brenner, S. Lodha, and S. Rajan, *Applied Physics Letters* **112**, 233503 (2018).
- ¹⁰ Z. Cheng, T. Bougher, T. Bai, S. Y. Wang, C. Li, L. Yates, B. Foley, M. S. Goorsky, B. A. Cola, and F. Faili, *ACS applied materials & interfaces* (2018).
- ¹¹ D. G. Cahill, *Review of scientific instruments* **75**, 5119 (2004).
- ¹² A. J. Schmidt, *Annual Review of Heat Transfer* **16** (2013).
- ¹³ Z. Cheng, T. Bai, Y. Wang, C. Li, K. D. Hobart, T. I. Feygelson, M. J. Tadjer, B. B. Pate, B. M. Foley, and L. Yates, arXiv preprint arXiv:1807.11400 (2018).
- ¹⁴ Z. Cheng, L. Yates, J. Shi, M. J. Tadjer, K. D. Hobart, and S. Graham, arXiv preprint arXiv:1901.02961 (2019).
- ¹⁵ P. Jiang, B. Huang, and Y. K. Koh, *Review of Scientific Instruments* **87**, 075101 (2016).
- ¹⁶ J. Liu, J. Zhu, M. Tian, X. Gu, A. Schmidt, and R. Yang, *Review of Scientific Instruments* **84**, 034902 (2013).
- ¹⁷ Z. Cheng, A. Weidenbach, T. Feng, M. B. Tellekamp, S. Howard, M. J. Wahila, B. Zivasatienraj, B. Foley, S. T. Pantelides, and L. F. Piper, *Physical Review Materials* **3**, 025002 (2019).
- ¹⁸ P. Jiang, X. Qian, X. Li, and R. Yang, *Applied Physics Letters* **113**, 232105 (2018).
- ¹⁹ Z. Guo, A. Verma, X. Wu, F. Sun, A. Hickman, T. Masui, A. Kuramata, M. Higashiwaki, D. Jena, and T. Luo, *Applied Physics Letters* **106**, 111909 (2015).
- ²⁰ M. D. Santia, N. Tandon, and J. Albrecht, *Applied Physics Letters* **107**, 041907 (2015).
- ²¹ J. Liu, Z. Xu, Z. Cheng, S. Xu, and X. Wang, *ACS applied materials & interfaces* (2015).
- ²² Z. Cheng, L. Liu, S. Xu, M. Lu, and X. Wang, *Scientific reports* **5** (2015).
- ²³ P. Martin, Z. Aksamija, E. Pop, and U. Ravaioli, *Physical review letters* **102**, 125503 (2009).
- ²⁴ Y. K. Koh, Y. Cao, D. G. Cahill, and D. Jena, *Advanced Functional Materials* **19**, 610 (2009).